



# Cored-wire arc spray fabrication of novel aluminium-copper coatings for anti-corrosion/fouling hybrid performances

Lijia Fang<sup>1</sup>, Jing Huang<sup>1</sup>, Yi Liu, Botao Zhang, Hua Li\*

Key Laboratory of Marine Materials and Related Technologies, Zhejiang Key Laboratory of Marine Materials and Protective Technologies, Ningbo Institute of Materials Technology and Engineering, Chinese Academy of Sciences, Ningbo 315201, China

## ARTICLE INFO

### Keywords:

Cored wires  
Arc spray  
Marine coating  
Copper biocides  
Antifouling

## ABSTRACT

The booming ocean economy in recent decades crucially demands advanced anti-corrosion technologies for marine infrastructures. Among the marine protective coatings developed in past decades, thermal sprayed aluminium coating was evidenced to be one of the most economical and efficient corrosion protection layers. Yet, marine corrosion is always accompanied by biofouling which in most cases accelerates corrosion. Here we report arc spray fabrication of novel aluminium-copper coatings using home-made Al-Cu cored wires for both anti-corrosion and antifouling performances. Copper particles were dispersed in the as-sprayed coatings, and TEM characterization further revealed partial interaction of Cu particles with Al matrix during the coating deposition. The chemical reaction with the formation of  $Al_2Cu$  offered an anchoring effect for the coatings preventing Cu particles from quick releasing into aqueous environment. Electrochemical testing in artificial seawater showed that the presence of Cu in Al coatings did not trigger considerable deterioration in corrosion resistance. Further antifouling testing of the coatings by examining settlement and colonization behaviors of bacteria *E. coli* and *Bacillus* sp. and typical marine algae revealed their excellent antifouling performances. The antifouling properties were predominately attributed to the continuous release of copper ions from the coatings. The results give clear insight into constructing anti-corrosion/fouling inorganic coatings by the cored-wire arc spray technical route for marine applications.

## 1. Introduction

Corrosion is one of the predominant worldwide concerns in modern marine industries, which impact on the service reliability of marine materials, causing substantial economic losses. Thermal spray has been proven to be an efficient surface protection technique, in particular in fabricating anti-corrosion coatings on marine materials surfaces [1–4]. Thermal sprayed metallic coatings, such as aluminium, zinc, and aluminium-zinc alloy coatings, were extensively used for marine corrosion protection. Owing to the cost-efficiency, light weight, and remarkable anti-corrosion properties [5], Al-based coatings performed well in corrosive environment for up to 30 years [6–8]. However, it should be noted that apart from the corrosion in the marine environment, marine biofouling is another major concern for marine infrastructures. Marine biofouling is a negative phenomenon brought about by adherence of marine microbes to the surfaces immersed in seawater [9]. Biofouling usually causes a variety of problems for instance reduced ship speed, increased fuel consumption of vessels, microbiologically induced

corrosion, and pipe clogging. Therefore appropriate measures must be taken for marine structures to combat biofouling [10]. In recent decades, many marine antifouling technologies have been widely explored [11], which were mainly related to organic painting [12,13]. For thermal sprayed marine coatings, to the best knowledge of the authors, few reports are available on thermal sprayed inorganic antifouling coatings.

The antifouling techniques based on use of biocides have been the most common method in modern marine industry [14]. However, most effective biocides have been banned for their environmental toxicity. Regardless of the fact that copper agents persist as the widely used biocide, such as copper compounds, cuprous oxide and copper alloys [15–17], excessive release of copper ions would inevitably cause unpredictable consequences for marine organisms. Long-term controlled release of copper from antifouling coatings is therefore one of the current research focuses for developing environment-friendly antifouling techniques. For marine applications, it is also essential that biocide-containing coating possesses both sufficient corrosion

\* Corresponding author.

E-mail address: [lihua@nimte.ac.cn](mailto:lihua@nimte.ac.cn) (H. Li).

<sup>1</sup> These authors contributed equally to this work.

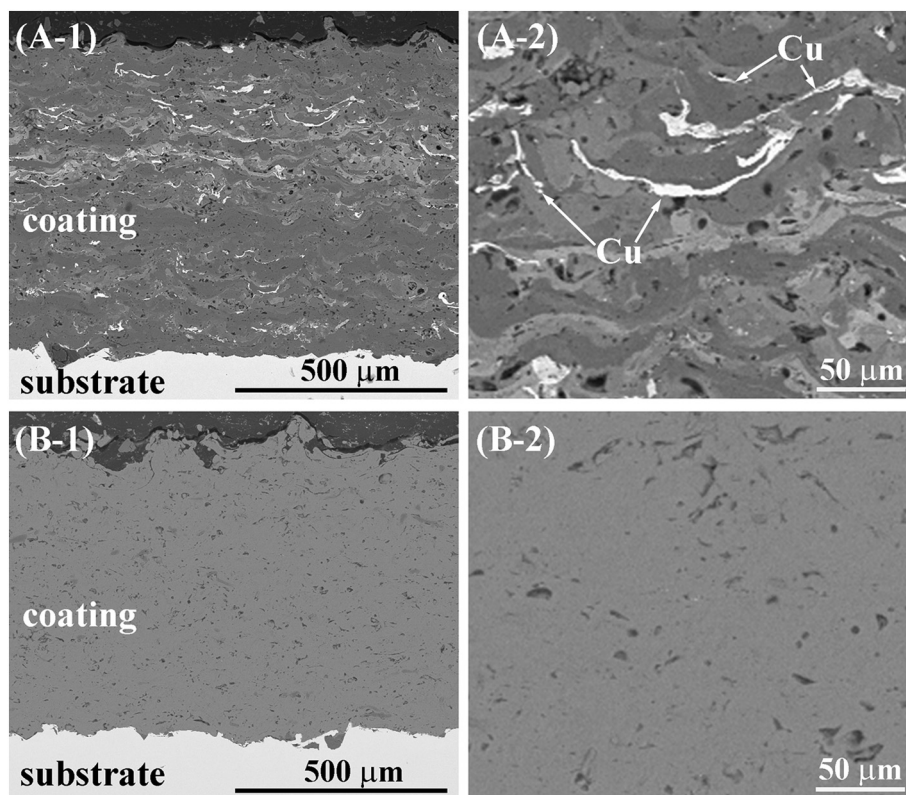


Fig. 1. Cross-sectional morphology of the Al-Cu coating (A-1, A-2) and the Al coating (B-1, B-2) (A-2 and B-2 are enlarged views of selected areas in A-1 and B-1, respectively).

resistance and sustained long-lasting antimicrobial release [16].

To accomplish the hybrid properties, new spray system and cored wires were both developed for making marine coatings [18]. Arc sprayed coatings using cored wires as the starting feedstock have already been widely used in many industrial applications [19]. Arc spray involves the use of two electrically conductive wires that are continuously fed into a common arc point at which a temperature of up to the melting temperature of the wire material is achieved. Twin-wires arc spray provides operational and economic advantages [20]. In this study, copper nanoparticles were used as antifouling agent and Al-Cu cored wires were employed for the arc spray coating deposition. Microstructure, corrosion resistance, and antifouling properties of the coatings were examined and elucidated.

## 2. Materials and methods

Aluminium-based cored wire (Al-Cu) with Cu nanoparticles as filler was used as the feedstock for the arc spraying, and the wire had the diameter of 2 mm (bandwidth of the aluminium velum: 7 mm, thickness of the velum: 400 μm). For the cored-wire preparation, the commercial spherical copper nanopowder with the diameter of 200–300 nm (Changsha Tianjiu Metal Materials Co. Ltd., China) was used as the inner filler, and the powder filling rate was ~26%. 316 stainless steel plates with the dimension of 30 mm × 20 mm × 1.5 mm were used as the substrates for the coating deposition. Before the spraying using the twin-wire arc spray system (Castolin-Eutectic Pte Ltd., Nashville, USA), the substrates were grit-blasted and cleaned in an ultrasonic ethanol bath. The voltage and current of the arc spray was 32 V and 100 A, respectively. Pressure of the compressed air was 0.65 MPa and the spraying distance was 150 mm. The robot controlled moving speed of the spray gun was 200 mm/s. For comparison purposes, solid aluminium wire was also sprayed using the same spray conditions.

Microstructure of the coatings was characterized by field emission

scanning electron microscope (FESEM, Quanta FEG 250, USA). Porosity of the coatings was measured using the image analysis software *ImageJ* and at least ten images were assessed for each coating. To examine the phase changes, sprayed particles were collected and analyzed, and the collection was made by directly spraying the droplets into room-temperature distilled water. It was a usual approach that distilled water or liquid nitrogen was used as the cooling media to collect the droplets for studying the phase transformation of sprayed materials during thermal spraying, since it was generally believed that the quenching of droplets is rapid upon their impingement on substrate/pre-coating. Size distribution of the sprayed particles was determined by a particle size analyzer (Microtrac, S3500-special, USA). Chemistry of the samples was characterized by X-ray diffraction (XRD, PANalytical X'pert Pro, the Netherlands) using Cu K $\alpha$  operated at 40 kV and 30 mA. Corrosion resistance of the coatings were tested by electrochemical testing and potentiodynamic polarization curves were acquired using a Solartron Modulab system (2100A, UK). The testing was carried out in artificial seawater (ASW) using 1 cm<sup>2</sup> area of the specimen as the working electrode, and platinum electrode was used as the counter electrode and saturated calomel electrode (SCE) was employed as the reference electrode. Prior to the electrochemical measurements, the samples were immersed in an ASW-containing aerobic chamber. The testing was repeated three times to ensure reproducibility.

To reveal the antifouling performances of the coatings, gram-negative *E. coli* (ATCC 25922) and gram-positive *Bacillus* sp. (MCCC 1A00791) bacteria were typically chosen for the testing following the protocol reported previously [21]. Bacterial adhesion and antibacterial rate were further evaluated. 2216E (CM 0471) media was prepared by dissolving 1 g beef extract, 1 g yeast extract, 5 g peptone, and 0.01 g FePO<sub>4</sub> in 1000 ml deionized water as carbon and energy sources for *Bacillus* sp. LB media were prepared by dissolving 10 g sodium chloride (NaCl), 5 g yeast extract and 10 g peptone in 1000 ml deionized water as energy sources for *E. coli*. The coating samples were immersed in

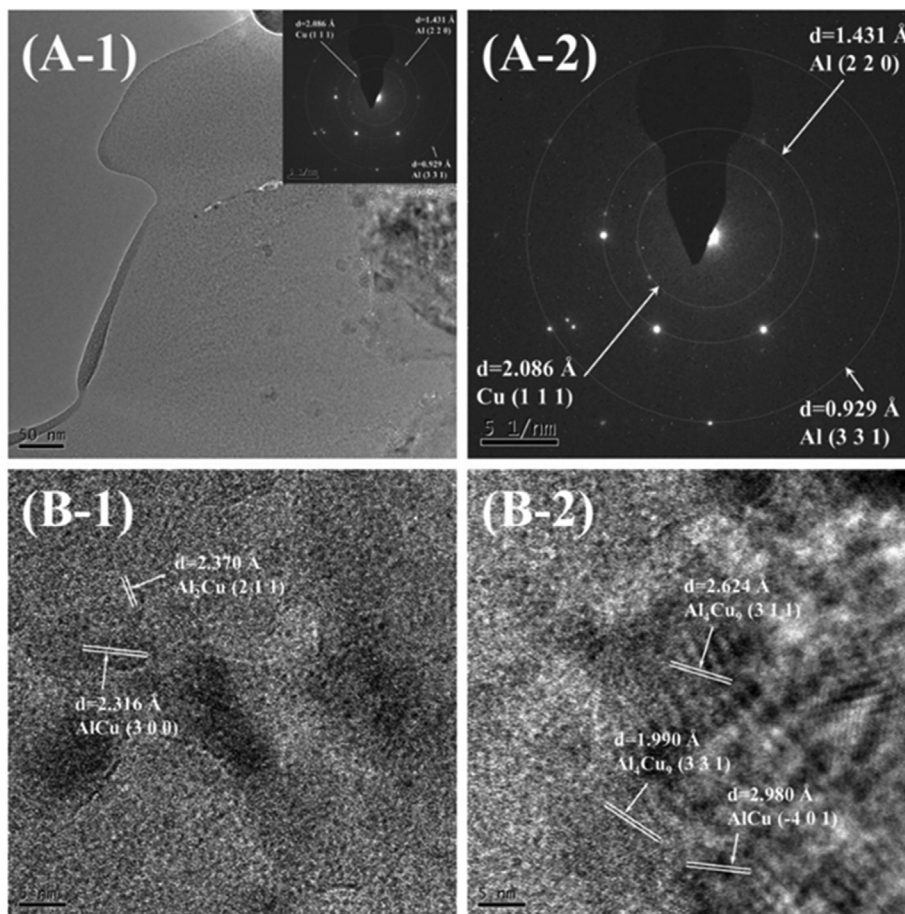


Fig. 2. TEM micrographs of the Al-Cu coating, (A-1) TEM image of the coating, (A-2) SAED pattern taken from the area shown in (A-1), and (B-1, B-2) HRTEM images of the coating.

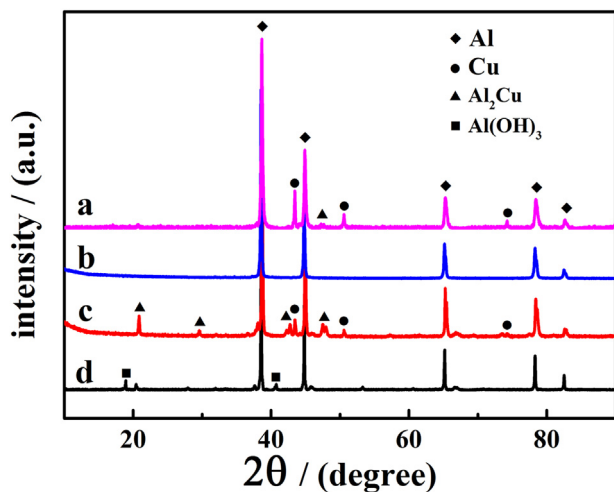


Fig. 3. XRD patterns of the as-sprayed Al-Cu coating (a), the as-sprayed Al coating (b), the as-sprayed Al-Cu powder (c), and the as-sprayed Al powder (d).

ASW containing the bacteria for 24 h at 25 °C. For FESEM observation, the bacteria after 24 h incubation were fixed in 2.5% glutaraldehyde for 2 h, and further dehydration and critical-point drying steps were conducted using a graded series of ethanol/water solutions. The algae *Phaeodactylum tricornutum* and *Chlorella* were typically employed in this study to further reveal the antifouling properties of the coatings. The microorganisms were cultured in ASW medium at 20 °C under aseptic conditions. Adhesion of the algae on the samples for 3 days was

characterized by confocal laser scanning microscopy (CLSM, TCS SP5, Germany). Releasing rate of copper ions from the coatings was measured in 3.5 wt% NaCl solution (up to 21 days) using an inductively coupled plasma optical emission spectrometer (ICP-OES, PE Optima 2100DV, Perkin-Elmer, USA).

### 3. Results and discussion

The coatings with dense structure were successfully fabricated by the high velocity arc spray (Fig. 1). No obvious cracking or spallation is seen for both the pure Al and the Al-Cu coatings, and the statistical porosity of 2.01% and 2.30% was obtained for the Al and the Al-Cu coating, respectively. It is clear that addition of Cu nanoparticles did not trigger obvious changes in porosity of Al coating. However, lamellar microstructural feature of the Al-Cu coating is more recognizable than the pure Al coating (Fig. 1A-2 vs. B-2). This is not surprising since it is clear that the Cu particles are located mainly at the interfaces of adjacent Al splats. The parts in white color refer to copper particles seen from the cross-sectional views of the coatings (Fig. 1A-1 and A-2). Clusters of copper nanoparticles are seen, which is likely due to melting/solidification-induced agglomeration of the particles during the coating deposition stage.

Further characterization by HRTEM revealed chemical interaction between Al and Cu during the spraying (Fig. 2). The SAD patterns of the Al-Cu coating suggest the presence of aluminium and copper in the coating (Fig. 2A-2). The diffraction patterns of  $d = 0.929 \text{ \AA}$  and  $d = 1.431 \text{ \AA}$  are assigned to the crystal face (3 3 1) and (2 2 0) of aluminium, respectively. The diffraction pattern of  $d = 2.086 \text{ \AA}$  is attributed to the crystal face (1 1 1) of copper [22]. The HRTEM pictures

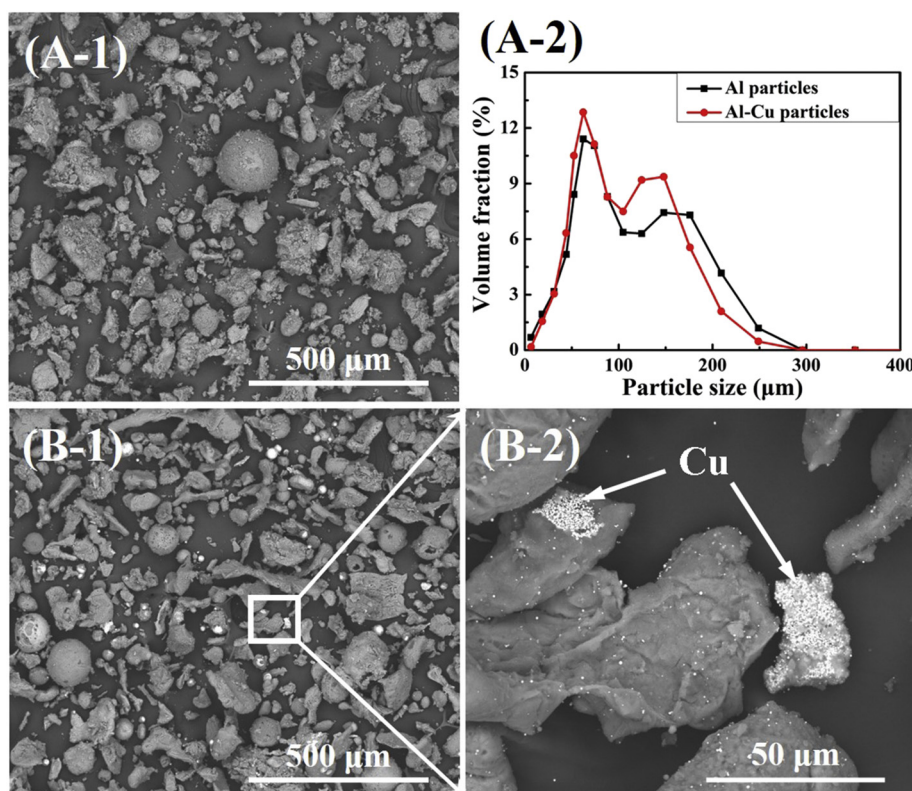


Fig. 4. Characteristics of the as-sprayed Al and Al-Cu particles collected by directly spraying the droplets into distilled water, (A-1) SEM picture of the as-sprayed Al particles, (B-1, B-2) SEM pictures of the as-sprayed Al-Cu particles, and (A-2) size distribution of the as-arc-sprayed particles. (For interpretation of the references to color in this figure, the reader is referred to the web version of this article.)

clearly show the presence of typical intermetallics of Cu and Al (Fig. 2B-1 and B-2).  $\text{Al}_2\text{Cu}$  grains grow along (2 1 1) plane and exhibit a lattice spacing of 2.370 Å. Moreover,  $\text{Al}_4\text{Cu}_9$  grains grow along (3 1 1) and (3 3 1) planes and AlCu grains grow along (3 0 0) and (−4 0 1) planes, showing the lattice spacing of 2.624 Å and 2.316 Å and 2.980 Å, respectively. The thermodynamic driving force for the growth of Al-Cu intermetallic compounds has been well discussed [23,24]. Interaction of Al with Cu usually results in formation of  $\text{Al}_2\text{Cu}$ , AlCu or  $\text{Al}_4\text{Cu}_9$  [25]. In this case, the detected Al-Cu intermetallics and Cu suggest partial involvement of Cu particles in the chemical reaction with Al, which would favor the fixation of the nanoparticles in Al matrix for enhanced anchoring effect.

XRD analyses further evidenced the interaction between Al and Cu during the coating deposition (Fig. 3). The Al-Cu coating exhibits weak XRD peaks for  $\text{Al}_2\text{Cu}$ , indicating minor chemical reaction of Al with nano-copper during the spraying, which is likely attributed to the limited in-flight time of the Al-Cu droplets before flattening/solidification upon impingement on pre-coating/substrate. In addition, the short duration experienced by the droplets at high temperatures also gives rise to negligible oxidation of Al or copper. Since the results did not provide direct evidence to show melting/unmelting state of the Cu particles during the spraying, further measures are to be taken to characterize the retained Cu in the coatings. To further study the physicochemical behaviors of the Al-Cu droplets during the spraying, the droplets were sprayed into distilled water and the sprayed particles were collected. It is surprisingly noted that  $\text{Al}_2\text{Cu}$  phase is clearly detected in the as-sprayed Al-Cu particles (Fig. 3), indicating the predominate occurrence of the chemical reaction during the in-flight stage. This in turn further indicates that upon impingement of the Al-Cu particles, the reaction would already terminate. It is not surprising that the  $\text{Al}_2\text{Cu}$  phase is more remarkably detected in the as-sprayed particles than in the coating, since the phase is predominately located on the surface of big Al particles. While in the Al-Cu coating, most of the Al-Cu interfaces are not exposed (less  $\text{Al}_2\text{Cu}$  is detectable by XRD). Due to the differences in the melting temperature, 660 °C for Al and 1083 °C for Cu, during the arc spray in this case, Al in the vast majority in the

composites got melted earlier and solidified later than Cu, which usually accounts for the phenomenon that  $\text{Al}_2\text{Cu}$  phase prefers to form in most cases [25].

To reveal the mixing state in the as-sprayed Al-Cu particles, further characterization was conducted. Size distribution of the collected powder was measured using a particle size analyzer. Both the powder particles collected from the Al-Cu and the Al wires are irregular, and show the D50 size of 65 μm (Fig. 4). Moreover, the copper nanoparticles clusters are clearly recognized (the light-colored parts in Fig. 4B-1 and B-2), and they are either embedded in aluminium matrix or well dispersed on the surface of aluminium particles (Fig. 4B-2). This can well explain the predominate presence of Cu particles at aluminium splats' interfaces (Fig. 1A-2). The favorable dispersal of the biocide would ultimately facilitate the antifouling functions of the coatings when used in the marine environment.

Antifouling performances of the coating were assessed by examining adhesion and colonization behaviors of the typically selected bacteria and algae. The Al-Cu coating showed remarkable capability to resist adhesion of the microorganisms (Fig. 5). It is clear that after being incubated in the *E. coli*-containing media for 8 h, the Al-Cu coating shows significantly constrained colonization of the bacteria. As the control samples, the bare 316L plate and the pure Al coating exhibited lots of *E. coli* colonies (Fig. 5A-1 and A-2), suggesting apparent biofouling on their surfaces. In contrast, inhibited colonization of the bacteria is seen on the surface of the Al-Cu coating (Fig. 5A-3). To more clearly examine the colonization phenomena of the bacteria on the surfaces of the coatings, both the pure Al and the Al-Cu coatings were surface polished prior to the biofouling testing. Similar trend was revealed for the settlement and colonization of *Bacillus* sp. on their surfaces (Fig. 5B-1 and B-2). After immersed in the *Bacillus* sp.-containing seawater for 24 h, the Al-Cu coating showed excellent antifouling performances (Fig. 5B-2), while the Al coating did not show antifouling functions (Fig. 5B-1). This is likely attributed to release of copper ions into the solution, which has been well established for Cu-containing antifouling layers [26–28]. Extensive studies have proposed a number of antifouling

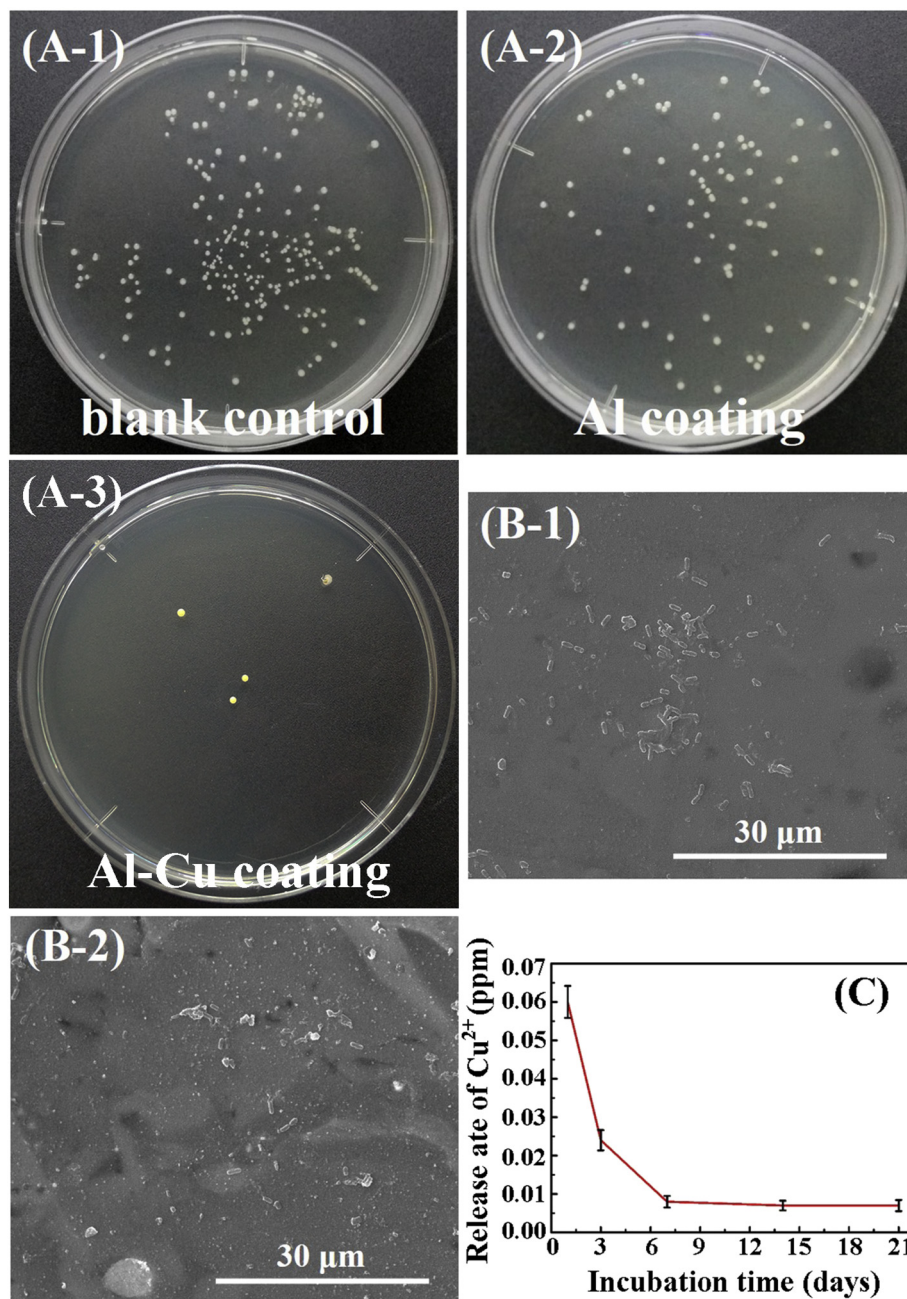


**Fig. 5.** Antibacterial performances of the samples against *E. coli* and *Bacillus* sp. (A) Digital photos of *E. coli* colonies in the blank sample (316L) Petri dish after 8 h incubation in *E. coli*-containing media (A-1), in the pure Al coating sample Petri dish after 8 h incubation in *E. coli*-containing media (A-2), and in the Al-Cu coating sample Petri dish after 8 h incubation in *E. coli*-containing media (A-3). (B-1, B-2) The colonization behaviors of *Bacillus* sp. on the Al coating (B-1) and the Al-Cu coating (B-2) after 24 h incubation in *Bacillus* sp. bacteria-containing ASW. (C) Release rate of copper ions from the Al-Cu coatings.

mechanisms of copper ions. It is usually believed that upon immersion in aqueous solution, copper dissolves from the coating and it becomes unstable ion  $\text{Cu}^+$ , and then  $\text{Cu}^+$  is quickly oxidized to more stable  $\text{Cu}^{2+}$ . Complex reactions of  $\text{Cu}^{2+}$  with inorganic and organic ligands result in formation of a reaction layer with a few microns thickness [26].  $\text{Cu}^{2+}$  adsorbed on cell surfaces can interact with cytoplasm and karyon of the bacteria, thereby destroying the function of bacterial enzymes or damaging cell membranes [29,30]. It is therefore essential that the effectiveness of biocides depends on their concentration (release rate) and exposure duration [31]. In this case, the concentration of copper ions released from the Al-Cu coating was measured using ICP-OES (Fig. 5C). After immersion of the coating in NaCl solution, the released dose of copper was relatively higher in the first three days,

0.06 ppm, and rapidly reduced to a relatively stable concentration value of  $\sim 0.008$  ppm (Fig. 5C). This could be well explained by the easy release of the copper particles existing on the top surface of the coating at early stage of incubation. Further release of the particles very much depends on the features of the Al-Cu composite structure. The anchoring of Cu particles by the chemical reaction of Al with Cu certainly restricts rapid release of the nanoparticles. A research has claimed that copper ions played a role in repelling the attachment of bacteria such as *Bacillus* sp., *E. coli*, when copper ion concentration reached 0.003 ppm [32]. In this study, it is interesting to note that aluminium matrix acts as binder to fix the copper nanoparticles, and in turn effectively controls their release into physiological media for long-term antifouling functions of the coatings.

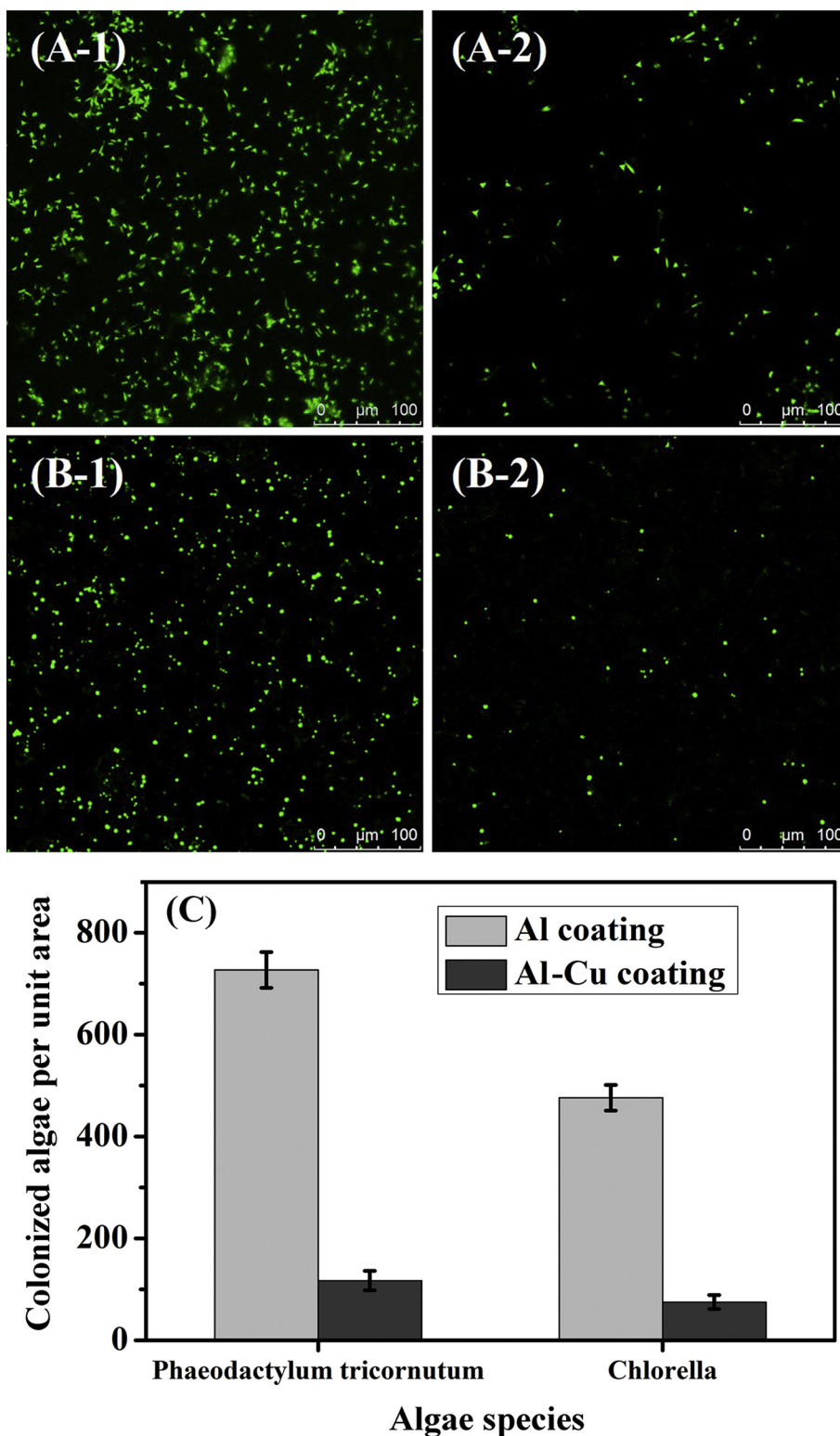


Fig. 6. CLSM images showing the colonization of *Phaeodactylum tricornutum* (A-1, A-2) and *Chlorella* (B-1, B-2) on the Al coating (A-1, B-1) and the Al-Cu coating (A-2, B-2) after 3 days incubation, and statistical analyses of the colonization (C).

Similar prohibited adhesion was also observed for the marine algae. After 3 days incubation in the media containing *Phaeodactylum tricornutum* or *Chlorella*, CLSM characterization of the Al-Cu coating showed that the addition of copper nanoparticles gave rise to effectively constrained colonization of the species (Fig. 6). For the Al coating, multiple layers of adhered algae and even their aggregation are seen (Fig. 6A-1 and B-1). Statistical analyses of the algal adhesion show that

after 3 days incubation, the Al-Cu coating exhibits significant decrease (~80%) in adhesion of *Phaeodactylum tricornutum* and *Chlorella* on its surface (Fig. 6C). Our previous study on the influence of  $Cu^{2+}$  on formation of conditioning layer and algae biofilm already revealed that the ions impacted on the cell membrane permeability of the microorganisms and regulated their EPS secretion [33]. The antifouling performances of the Al-Cu coating would benefit from the controlled release

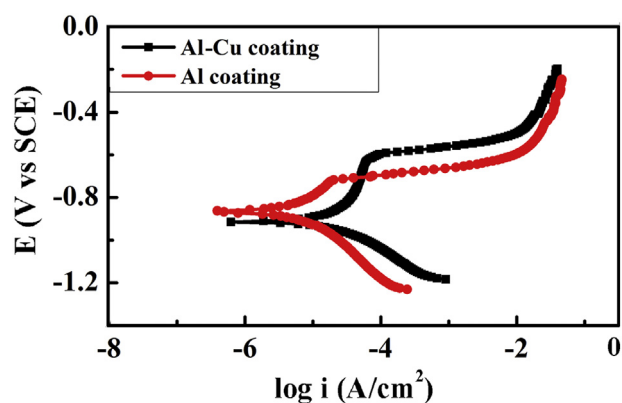


Fig. 7. Potentiodynamic polarization curves of the coatings tested in ASW.

Table 1

Polarization parameters of the coatings incubated in ASW.

Samples	$E_{corr}$ (V vs. SCE)	$i_{corr}$ (A/cm <sup>2</sup> )	$B_a$ (mV/decade)	$B_c$ (mV/decade)
Al coating	-0.8547	$1.250 \times 10^{-6}$	39.24	-74.64
Al-Cu coating	-0.8977	$4.639 \times 10^{-6}$	31.18	-79.32

of copper by the special composite structures.

The electrochemical testing suggested minor changes in corrosion resistance of the Al-Cu coating as compared to the Cu-free Al coating (Fig. 7). The electrochemical parameters, namely corrosion potential ( $E_{corr}$ ), corrosion current density ( $i_{corr}$ ), anodic Tafel slope ( $B_a$ ), and cathodic Tafel slope ( $B_c$ ), are listed in Table 1. The extrapolation of the anodic and cathodic Tafel lines gives the corrosion current density at the corrosion potential, and it should start 50–100 mV away from  $E_{corr}$  [21]. The  $E_{corr}$  and  $i_{corr}$  of -0.8977 V and  $4.639 \times 10^{-6}$  A/cm<sup>2</sup>, -0.8547 V and  $1.25 \times 10^{-6}$  A/cm<sup>2</sup>, were revealed for the Al-Cu coating and the Al coating, respectively. The higher corrosion current density exhibited by the Al-Cu coating is likely attributed to the co-existence of Cu with Al mainly at Al splats' interfaces. This is not surprising since the development of galvanic effects by contact between different metals usually causes galvanic corrosion [34], which triggers formation of a galvanic cell to accelerate corrosion of Al [35]. Additional EIS and salt fog testing also showed consistent anti-corrosion results (data not shown). Nevertheless, addition of the copper nanoparticles in Al coating well remains the promising corrosion resistance of Al, and offers the Al coating excellent antifouling properties. The cored-wire arc spray technical route sheds some light on developing novel anti-corrosion/fouling coatings for marine applications.

#### 4. Conclusions

A new cored-wire arc spray route was proposed for efficiently fabricating Al-Cu coatings and the Cu particles are dispersed mainly at Al splats' interfaces. The Cu nanoparticles partially take part in chemical reaction with Al, and the resultant intermetallics presumably facilitate anchoring of the nanoparticles against fast release into aqueous solution. Constrained releasing of Cu from the Al-Cu coating was revealed which gave rise to significant capability to resist colonization of typical bacteria *E. coli*, and *Bacillus* sp. and algae *Phaeodactylum tricornutum* and *Chlorella*. The addition of Cu nanoparticles did not obviously deteriorate the corrosion resistance of the Al coatings. The novel cost-effective arc sprayed Al-Cu coatings showed great potential for marine applications.

#### Acknowledgments

This research was supported by National Natural Science Foundation of China (grant # 41476064, 31500772, 21705158), Key Research and Development Program of Zhejiang Province (grant # 2015C01036), Zhejiang Provincial Natural Science Foundation of China (grant # LY18C100003), and International Scientific and Technological Cooperation Project of Ningbo (grant # 2017D10011).

#### Data availability

The raw/processed data required to reproduce these findings cannot be shared at this time as the data also forms part of an ongoing study.

#### References

- [1] J. Kawakita, T. Fukushima, S. Kuroda, T. Kodama, Corrosion behaviour of HVOF sprayed SUS316L stainless steel in seawater, *Corros. Sci.* 44 (2002) 2561–2581.
- [2] H.B. Choe, H.S. Lee, M.A. Ismail, M.W. Hussin, Evaluation of electrochemical impedance properties of anti-corrosion films by arc thermal metal spraying method, *Int. J. Electrochem. Sci.* 10 (2015) 9775–9789.
- [3] F. Ahnia, B. Demri, Evaluation of aluminum coatings in simulated marine environment, *Surf. Coat. Technol.* 220 (2013) 232–236.
- [4] D. Chaliampalias, G. Vourlias, E. Pavlidou, G. Stergioudis, S. Skolianos, K. Chrissafis, High temperature oxidation and corrosion in marine environments of thermal spray deposited coatings, *Appl. Surf. Sci.* 255 (2008) 3104–3111.
- [5] R. Rodriguez, R.S.C. Paredes, S.H. Wido, A. Calixto, Comparison of aluminum coatings deposited by flame spray and by electric arc spray, *Surf. Coat. Technol.* 202 (2007) 172–179.
- [6] F.S. Rogers, Thermal spray for commercial shipbuilding, *J. Therm. Spray Technol.* 6 (1997) 291–293.
- [7] R.J.K. Wood, A.J. Speyer, Erosion-corrosion of candidate HVOF aluminium-based marine coatings, *Wear* 256 (2004) 545–556.
- [8] S. Kuroda, J. Kawakita, M. Takemoto, An 18-year exposure test of thermal-sprayed Zn, Al, and Zn-Al coatings in marine environment, *Corrosion* 62 (2006) 635–647.
- [9] J.A. Callow, M.E. Callow, Trends in the development of environmentally friendly fouling-resistant marine coatings, *Nat. Commun.* 2 (2011) 244.
- [10] I. Banerjee, R.C. Pangule, R.S. Kane, Antifouling coatings: recent developments in the design of surfaces that prevent fouling by proteins, bacteria, and marine organisms, *Adv. Mater.* 23 (2011) 690–718.
- [11] P. Buskens, M. Wouters, C. Rentrop, Z. Vroon, A brief review of environmentally benign antifouling and foul-release coatings for marine applications, *J. Coat. Technol. Res.* 10 (2013) 29–36.
- [12] S.M. Olsen, L.T. Pedersen, M.H. Laursen, S. Kiil, K. Dam-Johansen, Enzyme-based antifouling coatings: a review, *Biofouling* 23 (2007) 369–383.
- [13] E. Almeida, T.C. Diamantino, O.D. Sousa, Marine paints: the particular case of antifouling paints, *Prog. Org. Coat.* 59 (2007) 2–20.
- [14] M. Thouvenin, J.J. Peron, C. Charreteur, P. Guerin, J.Y. Langlois, K. Vallee-Rehel, A study of the biocide release from antifouling paints, *Prog. Org. Coat.* 44 (2002) 75–83.
- [15] W.Y. Bao, O.O. Lee, H.C. Chung, M. Li, P.Y. Qian, Copper affects biofilm inducibility to larval settlement of the serpulid polychaete hydroids *elegans* (Haswell), *Biofouling* 26 (2010) 119–128.
- [16] D.M. Yebra, S. Kiil, K. Dam-Johansen, Antifouling technology - past, present and future steps towards efficient and environmentally friendly antifouling coatings, *Prog. Org. Coat.* 50 (2004) 75–104.
- [17] M.J. Vucko, P.C. King, A.J. Poole, C. Carl, M.Z. Jahedi, R. de Nys, Cold spray metal embedment: an innovative antifouling technology, *Biofouling* 28 (2012) 239–248.
- [18] H. Pokhmurska, V. Dovhnyuk, M. Student, E. Bielanska, E. Beltowska, Tribological properties of arc sprayed coatings obtained from FeCrB and FeCr-based powder wires, *Surf. Coat. Technol.* 151 (2002) 490–494.
- [19] R. Li, Z. Zhou, D.Y. He, Y.M. Wang, X. Wu, X.Y. Song, Microstructure and high temperature corrosion behavior of wire-arc sprayed FeCrSiB coating, *J. Therm. Spray Technol.* 24 (2015) 857–864.
- [20] P. Sheppard, H. Koiprasert, Effect of W dissolution in NiCrBSi-WC and NiBSi-WC arc sprayed coatings on wear behaviors, *Wear* 317 (2014) 194–200.
- [21] L. Abdoli, X.K. Suo, H. Li, Distinctive colonization of *Bacillus* sp. bacteria and the influence of the bacterial biofilm on electrochemical behaviors of aluminum coatings, *Colloids Surf. B* 145 (2016) 688–694.
- [22] C.H.N. Wei, Q.M. Liu, Shape-, size-, and density-tunable synthesis and optical properties of copper nanoparticles, *CrystEngComm* 19 (2017) 3254–3262.
- [23] Y.J. Guo, G.W. Liu, H.Y. Jin, Z.Q. Shi, G.J. Qiao, Intermetallic phase formation in diffusion-bonded Cu/Al laminates, *J. Mater. Sci.* 46 (2011) 2467–2473.
- [24] J. Chen, Y.S. Lai, Y.W. Wang, C.R. Kao, Investigation of growth behavior of Al-Cu intermetallic compounds in Cu wire bonding, *Microelectron. Reliab.* 51 (2011) 125–129.
- [25] H. Paul, L. Litynska-Dobrzynska, M. Prazmowski, Microstructure and phase constitution near the interface of explosively welded aluminum/copper plates, *Metall. Mater. Trans. A* 44 (2013) 3836–3851.
- [26] S. Ramesh, S. Rajeswari, Evaluation of inhibitors and biocide on the corrosion control of copper in neutral aqueous environment, *Corros. Sci.* 47 (2005) 151–169.

- [27] Y. Liu, X. Suo, Z. Wang, Y. Gong, X. Wang, H. Li, Developing polyimide-copper antifouling coatings with capsule structures for sustainable release of copper, *Mater. Des.* 130 (2017) 285–293.
- [28] J.L. Hobman, L.C. Crossman, Bacterial antimicrobial metal ion resistance, *J. Med. Microbiol.* 64 (2015) 471–497.
- [29] X. Zhang, K.E. Aifantis, Interpreting the softening of nanomaterials through gradient plasticity, *J. Mater. Res.* 26 (2011) 1399–1405.
- [30] J.Y. Yang, H. Xu, L.P. Zhang, Y. Zhong, X.F. Sui, Z.P. Mao, Lasting superhydrophobicity and antibacterial activity of Cu nanoparticles immobilized on the surface of dopamine modified cotton fabrics, *Surf. Coat. Technol.* 309 (2017) 149–154.
- [31] Y.Y. Zhu, Y.W. Ma, Q.J. Yu, J.X. Wei, J. Hu, Preparation of pH-sensitive core-shell organic corrosion inhibitor and its release behavior in simulated concrete pore solutions, *Mater. Des.* 119 (2017) 254–262.
- [32] A.K. Chatterjee, R.K. Sarkar, A.P. Chattopadhyay, P. Aich, R. Chakraborty, T. Basu, A simple robust method for synthesis of metallic copper nanoparticles of high antibacterial potency against *E. coli*, *Nanotechnology* 23 (2012) 085103.
- [33] X. He, L. Abdoli, H. Li, Participation of copper ions in formation of alginate conditioning layer: evolved structure and regulated microbial adhesion, *Colloids Surf. B* 162 (2018) 220–227.
- [34] C. Blanc, N. Pebere, B. Tribollet, V. Vivier, Galvanic coupling between copper and aluminium in a thin-layer cell, *Corros. Sci.* 52 (2010) 991–995.
- [35] H.X. Meng, N. Wang, Y.M. Dong, Z.L. Jia, L.J. Gao, Y.J. Chai, Influence of M-B (M = Fe, Co, Ni) on aluminum-water reaction, *J. Power Sources* 268 (2014) 550–556.